

# NEURAL SPATIO-TEMPORAL POINT PROCESSES

**Ricky T. Q. Chen\***

University of Toronto;  
Vector Institute

rtqichen@cs.toronto.edu

**Brandon Amos**

Facebook AI Research  
bda@fb.com

**Maximilian Nickel**

Facebook AI Research  
maxn@fb.com

## ABSTRACT

We propose a new class of parameterizations for spatio-temporal point processes which leverage Neural ODEs as a computational method and enable flexible, high-fidelity models of discrete events that are localized in continuous time and space. Central to our approach is a combination of recurrent continuous-time neural networks with two novel neural architectures, *i.e.*, Jump and Attentive Continuous-time Normalizing Flows. This approach allows us to learn complex distributions for both the spatial and temporal domain and to condition non-trivially on the observed event history. We validate our models on data sets from a wide variety of contexts such as seismology, epidemiology, urban mobility, and neuroscience.

## 1 INTRODUCTION

Modeling discrete events that are localized in continuous time and space is an important task in many scientific fields and applications. Spatio-temporal point processes (STPPs) are a versatile and principled framework for modeling such event data and have, consequently, found many applications in a diverse range of fields. This includes, for instance, modeling earthquakes and aftershocks (Ogata, 1988; 1998), the occurrence and propagation of wildfires (Hering et al., 2009), epidemics and infectious diseases (Meyer et al., 2012; Schoenberg et al., 2019), urban mobility (Du et al., 2016), the spread of invasive species (Balderama et al., 2012), and brain activity (Tagliazucchi et al., 2012).

It is of great interest in all of these areas to learn high-fidelity models which can jointly capture spatial and temporal dependencies and their propagation effects. However, existing parameterizations of STPPs are strongly restricted in this regard due to computational considerations: In its general form, STPPs require to solve multivariate integrals for computing likelihood values and thus have primarily been studied within the context of different approximations and model restrictions. This includes, for instance, restricting the model class to parameterizations with known closed-form solutions (*e.g.*, exponential Hawkes processes (Ozaki, 1979)), to restrict dependencies between the spatial and temporal domain (*e.g.*, independent and unpredictable marks (Daley & Vere-Jones, 2003)), or to discretize continuous time and space (Ogata, 1998). These restrictions and approximations—which can lead to mis-specified models and loss of information—motivated the development of neural temporal point processes such as Neural Hawkes Processes (Mei & Eisner, 2017) and Neural Jump SDEs (Jia & Benson, 2019). While these methods are more flexible, they can still require approximations such as Monte-Carlo sampling of the likelihood (Mei & Eisner, 2017; Nickel & Le, 2020) and, most importantly, only model restricted spatial distributions (Jia & Benson, 2019).

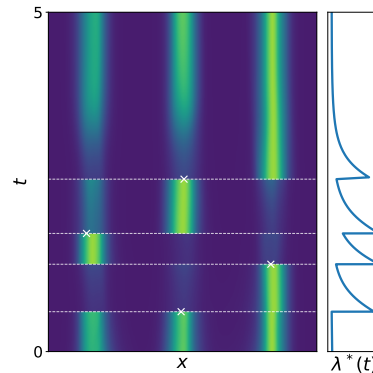


Figure 1: Color is used to denote  $p(x|t)$ , which can be evaluated exactly for Neural STPPs. After observing an event in one mode, the model is instantaneously updated as it strongly expects an event in the next mode. After a period of no observations, the model smoothly reverts back to the marginal distribution.

\*Work done while at Facebook AI Research.

To overcome these issues, we propose a new class of parameterizations for spatio-temporal point processes which leverage Neural ODEs as a computational method and allow to define flexible, high-fidelity models for spatio-temporal event data. We build upon ideas of Neural Jump SDEs (Jia & Benson, 2019) and Continuous-time Normalizing Flows (CNFs; Chen et al. 2018; Grathwohl et al. 2019; Mathieu & Nickel 2020) to learn parametric models of spatial (or mark<sup>1</sup>) distributions that are defined continuously in time. Normalizing flows are known to be flexible universal density estimators (e.g. Huang et al. 2018; 2020; Teshima et al. 2020; Kong & Chaudhuri 2020) while retaining computational tractability. As such, our approach allows the computation of exact likelihood values even for highly complex spatio-temporal distributions, and our models create smoothly changing spatial distributions that naturally benefits spatio-temporal modeling. Central to our approach, are two novel neural architectures based on CNFs—using either discontinuous jumps in distribution or self-attention—to condition spatial distributions on the event history. To the best of our knowledge, this is the first method that combines the flexibility of neural TPPs with the ability to learn high-fidelity models of continuous marks that can have complex dependencies on the event history. In addition to our modeling contributions, we also construct five new pre-processed data sets for benchmarking spatio-temporal event models.

## 2 BACKGROUND

In the following, we give a brief overview of two core frameworks which our method builds upon, *i.e.*, spatio-temporal point processes and continuous-time normalizing flows.

**Event Modeling with Point Processes** Spatio-temporal point processes are concerned with modeling sequences of random events in continuous space and time (Moller & Waagepetersen, 2003; Baddeley et al., 2007). Let  $\mathcal{H} = \{(t_i, \mathbf{x}_i)\}_{i=1}^n$  denote the sequence of event times  $t_i \in \mathbb{R}$  and their associated locations  $\mathbf{x}_i \in \mathbb{R}^d$ , the number of events  $n$  being also random. Additionally, let  $\mathcal{H}_t = \{(t_i, \mathbf{x}_i) \mid t_i < t, t_i \in \mathcal{H}\}$  denote the history of events predating time  $t$ . A spatio-temporal point process is then fully characterized by its *conditional intensity function*

$$\lambda(t, \mathbf{x} \mid \mathcal{H}_t) \triangleq \lim_{\Delta t \downarrow 0, \Delta \mathbf{x} \downarrow 0} \frac{\mathbb{P}(t_i \in [t, t + \Delta t], \mathbf{x}_i \in B(\mathbf{x}, \Delta \mathbf{x}) \mid \mathcal{H}_t)}{|B(\mathbf{x}, \Delta \mathbf{x})| \Delta t}. \quad (1)$$

where  $B(\mathbf{x}, \Delta \mathbf{x})$  denotes a ball centered at  $\mathbf{x} \in \mathbb{R}^d$  and with radius  $\Delta \mathbf{x}$ . The only condition is that  $\lambda(t, \mathbf{x} \mid \mathcal{H}_t) \geq 0$  and need not be normalized. Given  $i - 1$  previous events, the conditional intensity function describes therefore the instantaneous probability of the  $i$ -th event occurring at  $t$  and location  $\mathbf{x}$ . In the following, we will use the common star superscript shorthand  $\lambda^*(t, \mathbf{x}) = \lambda(t, \mathbf{x} \mid \mathcal{H}_t)$  to denote conditional dependence on the history. The joint log-likelihood of observing  $\mathcal{H}$  within a time interval of  $[0, T]$  is then given by (Daley & Vere-Jones, 2003, Proposition 7.3.III)

$$\log p(\mathcal{H}) = \sum_{i=1}^n \log \lambda^*(t_i, \mathbf{x}_i) - \int_0^T \int_{\mathbb{R}^d} \lambda^*(\tau, \mathbf{x}) d\mathbf{x} d\tau. \quad (2)$$

Training general STPPs with maximum likelihood is difficult as eq. (2) requires solving a multivariate integral. This need to compute integrals has driven research to focus around the use of kernel density estimators (KDE) with exponential kernels that have known anti-derivatives (Reinhart et al., 2018).

**Continuous-Time Normalizing Flows** Normalizing flows (Dinh et al., 2014; 2016; Rezende & Mohamed, 2015) is a class of density models that describe flexible distributions by parameterizing an invertible transformation from a simpler base distribution, which enables exact computation of the probability of the transformed distribution, without any unknown normalization constants.

Given a random variable  $\mathbf{x}_0$  with known distribution  $p(\mathbf{x}_0)$  and an invertible transformation  $T(\mathbf{x})$ , the transformed variable  $T(\mathbf{x}_0)$  is a random variable with a probability distribution function that satisfies

$$\log p(T(\mathbf{x}_0)) = \log p(\mathbf{x}_0) - \log \left| \det \frac{\partial T}{\partial \mathbf{x}}(\mathbf{x}_0) \right|. \quad (3)$$

There have been many advances in parameterizing  $T$  with flexible neural networks that also allow for cheap evaluations of eq. (3). We focus our attention on Continuous-time Normalizing Flows

<sup>1</sup>We regard any marked temporal point process with continuous marks as a spatio-temporal point process.

(CNFs), which parameterizes this transformation with a Neural ODE (Chen et al., 2018). CNFs define an infinite set of distributions on the real line that vary smoothly across time, and will be our core component for modeling events in the spatial domain.

Let  $p(\mathbf{x}_0)$  be the base distribution<sup>2</sup>. We then parameterize an instantaneous change in the form of an ordinary differential equation (ODE),  $\frac{d\mathbf{x}_t}{dt} = f(t, \mathbf{x}_t)$ , where the subscript denotes dependence on  $t$ . This function can be parameterized using any Lipschitz-continuous neural network. Conditioned on a sample  $\mathbf{x}_0$  from the base distribution, let  $\mathbf{x}_t$  be the solution of the initial value problem<sup>3</sup> at time  $t$ , i.e. it is from a trajectory that passes through  $\mathbf{x}_0$  at time 0 and satisfies the ODE  $\frac{d\mathbf{x}_t}{dt} = f$ . We can express the value of the solution at time  $t$  as

$$\mathbf{x}_t = \mathbf{x}_0 + \int_0^t f(\tau, \mathbf{x}_\tau) d\tau. \quad (4)$$

The distribution of  $\mathbf{x}_t$  then also continuously changes in  $t$  through the following equation,

$$\log p(\mathbf{x}_t|t) = \log p(\mathbf{x}_0) - \int_0^t \text{tr} \left( \frac{\partial f}{\partial \mathbf{x}}(\tau, \mathbf{x}_\tau) \right) d\tau. \quad (5)$$

In practice, eq. (4) and eq. (5) are solved together from 0 to  $t$ , as eq. (5) alone is not an ordinary differential equation but the combination of  $\mathbf{x}_t$  and  $\log p(\mathbf{x}_t)$  is. The trace of the Jacobian  $\frac{\partial f}{\partial \mathbf{x}}(\tau, \mathbf{x}_\tau)$  can be estimated using a Monte Carlo estimate of the identity (Skilling, 1989; Hutchinson, 1990),  $\text{tr}(A) = \mathbb{E}_{v \sim \mathcal{N}(0,1)}[v^\top A v]$ . This estimator relies only on a vector-Jacobian product, which can be efficiently computed in modern automatic differentiation and deep learning frameworks. This has been used (Grathwohl et al., 2019) to scale CNFs to higher dimensions using a Monte Carlo estimate of the log likelihood objective,

$$\log p(\mathbf{x}_t|t) = \log p(\mathbf{x}_0) - \mathbb{E}_{v \sim \mathcal{N}(0,1)} \left[ \int_0^t v^\top \frac{\partial f}{\partial \mathbf{x}}(\tau, \mathbf{x}_\tau) v d\tau \right], \quad (6)$$

which, even if only one sample of  $v$  is used, is still amenable to training with stochastic gradient descent. Gradients with respect to any parameters in  $f$  can be computed with constant memory by solving an adjoint ODE in reverse-time as described in Chen et al. (2018).

### 3 NEURAL SPATIO-TEMPORAL POINT PROCESSES

We are interested in modeling high-fidelity distributions in continuous time and space that can be updated based on new event information. For this purpose, we use the Neural ODE framework to parameterize a STPP by combining ideas from Neural Jump SDEs and Continuous Normalizing Flows to create highly flexible models that still allow exact likelihood computation.

We first (re-)introduce necessary notation. Let  $\mathcal{H} = \{(t_i, \mathbf{x}_{t_i}^{(i)})\}$  denote a sequence of event times  $t_i \in [0, T]$  and locations  $\mathbf{x}_{t_i}^{(i)} \in \mathbb{R}^d$ . The superscript indicates an association with the  $i$ -th event, and the use of subscripting with  $t_i$  will be useful later in the continuous-time modeling framework. Following Daley & Vere-Jones (2003), we decompose the conditional intensity function as

$$\lambda^*(t, \mathbf{x}) = \lambda^*(t) p^*(\mathbf{x} | t) \quad (7)$$

where  $\lambda^*(t)$  is the *ground intensity* of the temporal process and where  $p^*(\mathbf{x} | t)$  is the *conditional density* of a mark  $\mathbf{x}$  at  $t$  given  $\mathcal{H}_t$ . The star superscript is used as again shorthand to denote dependence on the history. Since  $\int_{\mathbb{R}^d} p^*(\mathbf{x} | t) = 1$ , eq. (7) allows us now to simplify the log-likelihood function of the joint process from eq. (2), such that

$$\log p(\mathcal{H}) = \underbrace{\sum_{i=1}^n \log \lambda^*(t_i) - \int_0^T \lambda^*(\tau) d\tau}_{\text{temporal log-likelihood}} + \underbrace{\sum_{i=1}^n p^*(\mathbf{x}_{t_i}^{(i)} | t_i)}_{\text{spatial log-likelihood}} \quad (8)$$

<sup>2</sup>This can be any distribution that is easy to sample from and evaluate log-likelihood for. We use the typical choice of a standard Normal in our experiments.

<sup>3</sup>This initial value problem has a unique solution if  $f$  is Lipschitz-continuous along the trajectory to  $\mathbf{x}_t$ , by the Picard–Lindelöf theorem.

Furthermore, based on eq. (7), we can derive separate models for the ground intensity and conditional mark density which will be jointly conditioned on a continuous-time hidden state with jumps. In the following, we will first describe how we construct a latent dynamics model, which we use to compute the ground intensity  $\lambda^*(t)$ . We will then propose three novel CNF-based approaches for modeling the conditional mark density  $p^*(\mathbf{x}|t)$ . We will first describe an unconditional model, which is already a strong baseline when spatial event distributions only follow temporal patterns and there is little to no correlation between the spatial observations. We then devise two new methods of conditioning on the event history  $\mathcal{H}$ : one explicitly modeling instantaneous changes in distribution, and another that uses an attention mechanism which is more amenable to parallelism.

**Latent Dynamics and Ground Intensity** For the temporal variables  $\{t_i\}$ , we follow the work of Jia & Benson (2019) and parameterize the intensity function using hidden state dynamics with jumps. Specifically, we evolve a continuous-time hidden state  $\mathbf{h}$  and set

$$\lambda^*(t) = g_\lambda(\mathbf{h}_t) \quad (\text{Ground intensity}) \quad (9)$$

where  $g_\lambda$  is a neural network with a softplus nonlinearity applied to the output, to ensure the intensity is positive. We then capture conditional dependencies through the use of a continuously changing state  $\mathbf{h}_t$  with instantaneous updates when conditioned on an event. The architecture is analogous to a recurrent neural network with a continuous-time hidden state (Rubanova et al., 2019). This provides us with a vector representation  $\mathbf{h}_t$  at every time value  $t$  that acts as both a summary of the history of events and as a predictor of future behavior. Instantaneous updates to  $\mathbf{h}_t$  allow to incorporate abrupt changes to the hidden state that are triggered by observed events. This mechanism is important for modeling TPPs and allows past events to influence future dynamics in a discontinuous way (e.g., modeling immediate shocks to a system).

We use  $f_h$  to model the continuous change in the form of an ODE and  $g_h$  to model instantaneous changes based on an observed event.

$$\mathbf{h}_{t_0} = \mathbf{h}_0 \quad (\text{An initial hidden state}) \quad (10)$$

$$\frac{d\mathbf{h}_t}{dt} = f_h(t, \mathbf{h}_t) \quad \text{between event times} \quad (\text{Continuous evolution}) \quad (11)$$

$$\lim_{\varepsilon \rightarrow 0} \mathbf{h}_{t_i + \varepsilon} = g_h(t_i, \mathbf{h}_{t_i}, \mathbf{x}_{t_i}^{(i)}) \quad \text{at event times } t_i \quad (\text{Instantaneous updates}) \quad (12)$$

The use of  $\varepsilon$  is to portray that  $\mathbf{h}_t$  is a *càglàd* function, i.e. left-continuous with right limits, with a discontinuous jump modeled by  $g_h$ .

The parameterization of continuous-time hidden states in the form of eqs. (10) to (12) has been used for time series modeling (Rubanova et al., 2019; De Brouwer et al., 2019) as well as TPPs (Jia & Benson, 2019). We parameterize  $f_h$  as a standard multi-layer fully connected neural network, and use the GRU update (Cho et al., 2014) to parameterize  $g_h$ , as was done in Rubanova et al. (2019).

**Time-varying CNF** The first model we consider is a straightforward application of the CNF to time-variable observations. Assuming that the spatial distribution is independent of prior events,

$$\log p^*(\mathbf{x}_{t_i}^{(i)}|t_i) = \log p(\mathbf{x}_{t_i}^{(i)}|t_i) = \log p(\mathbf{x}_{t_b}^{(i)}) - \int_{t_b}^{t_i} \text{tr} \left( \frac{\partial f}{\partial \mathbf{x}}(\tau, \mathbf{x}_\tau^{(i)}) \right) d\tau \quad (13)$$

where  $\mathbf{x}_\tau^{(i)}$  is the solution of the ODE  $f$  with initial value  $\mathbf{x}_{t_b}^{(i)}$ , the observed event location, at  $\tau = t_i$ , the observed event time. We set a base distribution at a fixed negative time value  $t_b$  to model an expressive distribution at time 0. The spatial distribution of an event modeled by a Time-varying CNF changes with respect to the time it occurs. Some spatio-temporal data sets exhibit mostly temporal patterns and little to no dependence on previous events in the spatial domain, which would make a time-varying CNF a good fit. Nevertheless, this model lacks the ability to capture spatial propagation effects, as it does not condition on previous event observations.

A major benefit of this model is the ability to evaluate the joint log-likelihood fully in parallel across events, since there are no dependencies between events. Most modern ODE solvers that we are aware of only allow a scalar terminal time. Thus, to solve all  $n$  integrals in eq. (13) with a single call to an ODE solver, we can simply reparameterize all integrals with a consistent dummy variable and track

the terminal time in the state. The joint ODE we use after the change of variables is

$$\frac{d}{ds} \underbrace{\begin{bmatrix} \mathbf{x}_s^{(0)} \\ \vdots \\ \mathbf{x}_s^{(n)} \end{bmatrix}}_{A_s} = \underbrace{\begin{bmatrix} st_0 f(st_0, \mathbf{x}_s^{(0)}) \\ \vdots \\ st_n f(st_n, \mathbf{x}_s^{(n)}) \end{bmatrix}}_{f(s, A_s)} \quad \text{which gives} \quad \underbrace{\begin{bmatrix} \mathbf{x}_0^{(0)} \\ \vdots \\ \mathbf{x}_0^{(n)} \end{bmatrix}}_{A_0} + \int_0^1 f(s, A_s) ds = \underbrace{\begin{bmatrix} \mathbf{x}_{t_0}^{(0)} \\ \vdots \\ \mathbf{x}_{t_n}^{(n)} \end{bmatrix}}_{A_1}. \quad (14)$$

Thus the full trajectories between 0 to  $t_i$  for all events can be computed in parallel using this augmented ODE by simply integrating once from  $s = 0$  to  $s = 1$ .

**Jump CNF** For the second model, we condition the dynamics defining the continuous normalizing flow on the hidden state  $\mathbf{h}$ , allowing the normalizing flow to update its distribution based on changes in  $\mathcal{H}$ . For this purpose, we define continuous-time spatial distributions by making again use of two components: (i) a continuous-time normalizing flow that evolves the distribution continuously, and (ii) a standard (discrete-time) flow model that changes the distribution instantaneously after conditioning on new events. As normalizing flows parameterize distributions through transformations of the samples, these continuous- and discrete-time transformations are composable in a straightforward manner and are end-to-end differentiable.

The generative process of a single event in a Jump CNF is given by:

$$\mathbf{x}_0 \sim p(\mathbf{x}_0) \quad (\text{An initial distribution}) \quad (15)$$

$$\frac{d\mathbf{x}_t}{dt} = f_x(t, \mathbf{x}_t, \mathbf{h}_t) \quad \text{between event times} \quad (\text{Continuous evolution}) \quad (16)$$

$$\lim_{\varepsilon \rightarrow 0} \mathbf{x}_{t_i + \varepsilon} = g_x(t_i, \mathbf{x}_{t_i}, \mathbf{h}_{t_i}) \quad \text{at event times } t_i \quad (\text{Instantaneous updates}) \quad (17)$$

The initial distribution can be parameterized by a normalizing flow. In practice, we set a base distribution at a negative time value and model  $p(\mathbf{x}_0)$  using the same CNF parameterized by  $f_x$ . The instantaneous updates (or jumps) describe conditional updates in distribution after each new event has been observed. This conditioning on  $\mathbf{h}_{t_i}$  is required for the continuous and instantaneous updates to depend on the history of observations. Otherwise, a Jump CNF would only be able to model the marginal distribution and behave similarly to a time-varying CNF. We solve for  $\mathbf{h}_t$  alongside  $\mathbf{x}_t$ .

The final probability of an event  $\mathbf{x}_t$  at some  $t > t_n$  after observing  $n$  events is given by the sum of changes according to the continuous- and discrete-time normalizing flows.

$$\begin{aligned} \log p^*(\mathbf{x}_t|t) &= \log p(\mathbf{x}_0) \\ &+ \underbrace{\sum_{t_i \in \mathcal{H}_t} \left( - \int_{t_{i-1}}^{t_i} \text{tr} \left( \frac{\partial f(\tau, \mathbf{x}_\tau, \mathbf{h}_\tau)}{\partial \mathbf{x}} \right) d\tau - \log \left| \det \frac{\partial g_x(t_i, \mathbf{x}_{t_i}, \mathbf{h}_{t_i})}{\partial \mathbf{x}} \right| \right)}_{\text{Change in density up to last event}} \\ &+ \underbrace{\int_{t_n}^t -\text{tr} \left( \frac{\partial f(\tau, \mathbf{x}_\tau, \mathbf{h}_\tau)}{\partial \mathbf{x}} \right) d\tau}_{\text{Change in density from last event to } t} \end{aligned} \quad (18)$$

As the instantaneous updates must be applied sequentially in a Jump CNF, we can only compute the integrals in eq. (18) one at a time. As such, the number of initial value problems scales linearly with the number of events in the history because the ODE solver must be restarted between each instantaneous update to account for the discontinuous change to state. This incurs a substantial cost when the number of events is large.

**Attentive CNF** To design a spatial model with conditional dependencies that alleviates the computational issues of Jump CNFs and can be computed in parallel, we make use of efficient attention mechanisms based on the Transformer architecture (Vaswani et al., 2017). Denoting only the spatial variables for simplicity, each conditional distribution  $\log p(\mathbf{x}_{t_i} | \mathcal{H}_{t_i})$  can be modeled by a CNF that depends on the sample path of prior events. Specifically, we take the dummy-variable reparameterization of eq. (14) and modify it so that the  $i$ -th event depends on all previous events using a Transformer

architecture for  $f$ ,

$$\frac{d}{ds} \begin{bmatrix} \mathbf{x}_s^{(0)} \\ \mathbf{x}_s^{(1)} \\ \vdots \\ \mathbf{x}_s^{(n)} \end{bmatrix} = \begin{bmatrix} st_0 f(st_0, \mathbf{x}_s^{(0)}, \mathbf{h}_{t_0}) \\ st_0 f(st_0, \mathbf{x}_s^{(0)}, \mathbf{x}_s^{(1)}, \mathbf{h}_{t_1}) \\ \vdots \\ st_n f(st_n, \mathbf{x}_s^{(0)}, \mathbf{x}_s^{(1)}, \dots, \mathbf{x}_s^{(n)}, \mathbf{h}_{t_n}) \end{bmatrix} := f_{\text{Attn}}. \quad (19)$$

With this formulation, the trajectory of  $\mathbf{x}_\tau^{(i)}$  depends continuously on the trajectory of  $\mathbf{x}_\tau^{(j)}$  for all  $j < i$  and the hidden state  $\mathbf{h}$ . Similar to eq. (14), an Attention CNF can now solve for the trajectories of all events in parallel but simultaneously depend non-trivially on  $\mathcal{H}$ .

To parameterize  $f_{\text{Attn}}$ , we use an embedding layer followed by two multihead attention (MHA) blocks and an output layer to map back into the input space. We use the Lipschitz-continuous multihead attention from Kim et al. (2020) as they recently showed that the dot product multihead attention (Vaswani et al., 2017) is not Lipschitz-continuous and thus may be ill-suited for parameterizing ODEs.

*Low-variance Log-likelihood Estimation* The variance of the Hutchinson stochastic trace estimator in eq. (6) grows with the squared Frobenius norm of the Jacobian,  $\sum_{ij} [\partial f / \partial x]_{ij}^2$  (Hutchinson, 1990). For attentive CNFs, we can remove some of the non-diagonal elements of the Jacobian and achieve a lower variance estimator. The attention mechanism creates a block-triangular Jacobian, where each block corresponds to one event, but the elements outside of the block-diagonal are solely due to the multihead attention. By *detaching the gradient connections* between different events in the MHA blocks, we can create a surrogate Jacobian matrix that do not contain cross-event partial derivatives. This effectively allows us to apply Hutchinson’s estimator on a matrix that has the same diagonal elements as the Jacobian  $\partial f / \partial x$ —and thus has the same expected value—but has zeros outside of the block-diagonal, leading to a lower variance trace estimator. The procedure consists of selectively removing partial derivatives and is straightforward but notationally cumbersome; the interested reader can find the details in Appendix E.

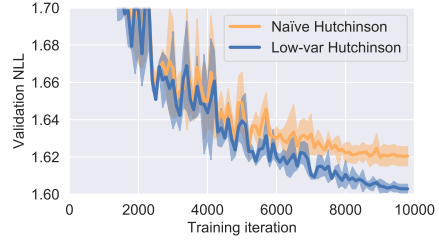


Figure 2: Lower variance estimates of the log-likelihood allows training better Attentive CNFs.

## 4 RELATED WORK

**Neural Temporal Point Processes** Modeling real-world data using restricted models such as Exponential Hawkes Processes (Ozaki, 1979) may lead to poor results due to model mis-specification. This motivated a variety of recent works to explore neural networks for the parameterization of TPPs. A common approach is to use recurrent neural networks to accumulate the event history in a latent state from which the intensity value can then be derived. Models of this form include, for instance, Recurrent Marked Temporal Point Processes (RMTPPs; Du et al. 2016) and Neural Hawkes Processes (NHPs; Mei & Eisner 2017). In contrast to our approach, these methods can not compute the exact likelihood of the model and have to resort to Monte-Carlo sampling for its approximation. However, this approach is especially problematic for commonly occurring clustered and bursty event sequences as it either requires a very high sampling rate or ignores important temporal dependencies (Nickel & Le, 2020). To overcome this issue, Jia & Benson (2019) proposed recently Neural Jump SDEs which extend the Neural ODE framework and allow to compute the exact likelihood for neural TPPs. This method is closely related to our approach and we build on its ideas to compute the ground intensity of the STPP. However, current Neural Jump SDEs—as well as NHPs and RMTPPs—are not well-suited for modeling complex *continuous* mark distributions as they are restricted to methods such as Gaussian mixture models in the spatial domain. Finally, Shchur et al. (2019); Mehrasa et al. (2019) considered to combine TPPs and CNFs, however for different purposes as in our case, *i.e.*, for intensity-free learning of TPPs.

**Continuous Normalizing Flows** The ability to describe an infinite number of distributions with a Continuous Normalizing Flow has been used by a few recent works. Some works in computer



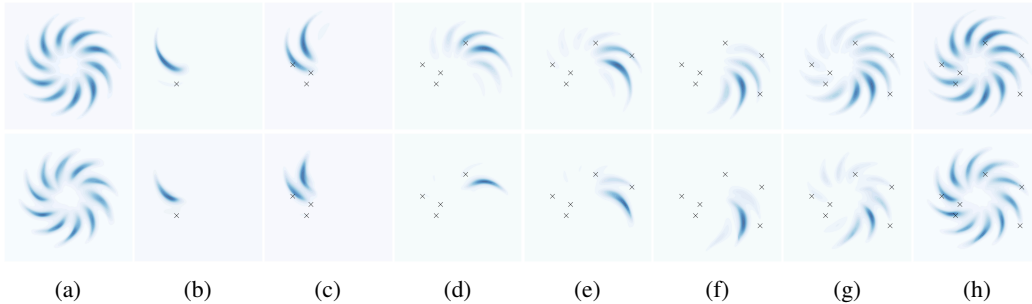


Figure 4: Evolution of spatial densities on Pinwheel data. *top*: Attentive CNF. *bottom*: Jump CNF. (a) Before observing any events, the distribution is even across all clusters. (b-f) Each event increases the probability of observing a future event from the subsequent cluster in clock-wise ordering. (g-h) After a period of no new events, the distribution smoothly returns back to the initial distribution (a).

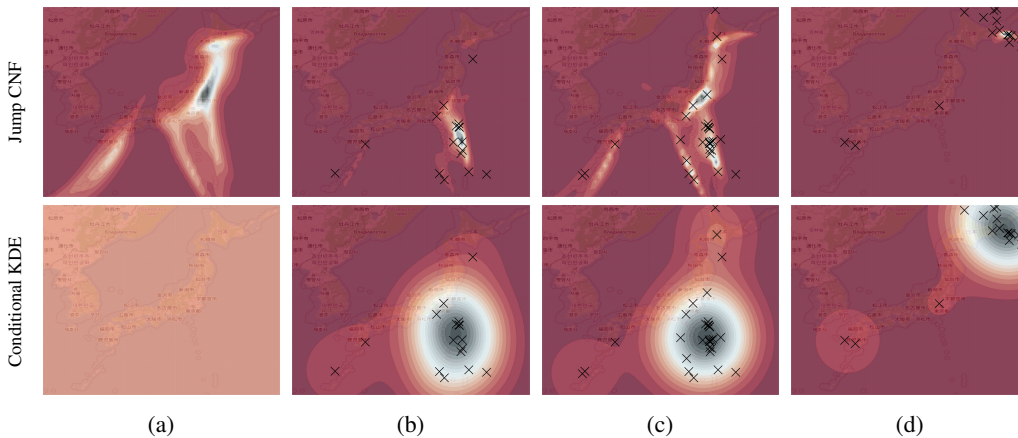


Figure 6: Snapshots of conditional spatial distributions modeled by the Jump CNF (*top*) and a conditional kernel density estimator (KDE; *bottom*). (a) Distribution before any events. (b-d) The Jump CNF’s distributions concentrate around tectonic plate boundaries where earthquakes and aftershocks gather, whereas the KDE has a large entropy in order to capture propagation of aftershocks.

graphics have used the interpolation effect of CNFs to model transformations of point clouds (Yang et al., 2019; Rempe et al., 2020; Li et al., 2020). CNFs have also been used in sequential latent variable models (Deng et al., 2020; Rempe et al., 2020). However, such works do not align the “time” axis of the CNF with the temporal axis of observations, and do not train on observations at more than one value of “time” in the CNF. In contrast, we align the time axis of the CNF with the time of the observations, directly using its ability to model distributions on a real-valued axis. A closely related application of CNFs to spatio-temporal data was done by Tong et al. (2020), who modeled the distribution of cells in a developing human embryo system at five fixed time values. In contrast to this, we extend to applications where observations are made at arbitrary time values and further jointly model such distributions with a temporal time process. Furthermore, Mathieu & Nickel (2020); Lou et al. (2020) recently proposed extensions of CNFs to Riemannian manifolds. For our proposed approach, this is especially interesting in the context of earth and climate science, as it allows us to model STPPs on the sphere simply by replacing the CNF with its Riemannian equivalent.

## 5 EXPERIMENTS

**Data Sets** As the world naturally moves along a temporal axis, many data sets can be represented as spatio-temporal events. We pre-process data from open sources and make them suitable for spatio-temporal event modeling. Varying across a wide range of domains, the data sets we consider are: earthquakes, pandemic spread, consumer demand for a bike sharing app, and high-amplitude brain

Model	Pinwheel		Earthquakes JP		COVID-19 NJ		BOLD5000	
	Temporal	Spatial	Temporal	Spatial	Temporal	Spatial	Temporal	Spatial
Poisson Process	-0.787 $\pm$ 0.020	–	-0.111 $\pm$ 0.001	–	0.878 $\pm$ 0.016	–	0.862 $\pm$ 0.018	–
Self-correcting Process	-2.115 $\pm$ 0.172	–	-7.051 $\pm$ 0.780	–	-10.053 $\pm$ 1.150	–	-6.470 $\pm$ 0.827	–
Hawkes Process	-0.239 $\pm$ 0.043	–	0.114 $\pm$ 0.005	–	2.092 $\pm$ 0.023	–	2.860 $\pm$ 0.050	–
Conditional KDE	–	-2.965 $\pm$ 0.008	–	-2.259 $\pm$ 0.001	–	-2.583 $\pm$ 0.000	–	-3.467 $\pm$ 0.000
Time-varying CNF	–	-2.201 $\pm$ 0.003	–	-1.459 $\pm$ 0.016	–	-2.002 $\pm$ 0.002	–	-1.846 $\pm$ 0.019
Neural Jump SDE (GRU)	-0.006 $\pm$ 0.042	-2.077 $\pm$ 0.026	0.186 $\pm$ 0.005	-1.652 $\pm$ 0.012	2.251 $\pm$ 0.004	-2.214 $\pm$ 0.005	5.675 $\pm$ 0.003	0.743 $\pm$ 0.089
Jump CNF	0.027 $\pm$ 0.002	-1.605 $\pm$ 0.009	0.166 $\pm$ 0.001	-1.007 $\pm$ 0.050	2.242 $\pm$ 0.002	-1.904 $\pm$ 0.004	5.536 $\pm$ 0.016	1.246 $\pm$ 0.185
Attentive CNF	0.034 $\pm$ 0.001	-1.572 $\pm$ 0.002	0.204 $\pm$ 0.001	-1.237 $\pm$ 0.075	2.258 $\pm$ 0.002	-1.864 $\pm$ 0.001	5.842 $\pm$ 0.005	1.252 $\pm$ 0.026

Table 1: Log-likelihood on held-out test data (higher is better). Standard devs. are computed over three runs.

signals from fMRI scans. We briefly describe these data sets here; further details and pre-processing steps can be found in Appendix C.

**PINWHEEL** This is a synthetic data set with multimodal and non-Gaussian spatial distributions designed to test the ability to capture fast changes due to event history (see fig. 4). The data set consists of 10 clusters which form a pinwheel structure. Events are sampled from a multivariate Hawkes process such that events from one cluster will drastically increase the probability of observing events in the next cluster following a clock-wise rotation.

**EARTHQUAKES** For modeling earthquakes and aftershocks, we gathered location and time of all earthquakes in Japan from 1990 to 2020 with magnitude of at least 2.5 from the [U.S. Geological Survey \(2020\)](#). We split the data into individual sequences using sliding windows of length 30 days.

**COVID-19 CASES** We use data released publicly by [The New York Times \(2020\)](#) on daily COVID-19 cases in New Jersey state, from March to July of 2020. The data is aggregated at the county level, which we dequantize uniformly across the county. We also dequantize the temporal axis by assigning new cases uniformly within the day. We split the data into sliding windows of 7 days.

**BOLD5000** This data consists of fMRI scans of 4 participants as they are given visual stimuli ([Chang et al., 2019](#)). We use the sessions of a single patient and convert brain responses into spatio-temporal events following the z-score thresholding approach in [Tagliazucchi et al. \(2012; 2016\)](#).

In addition to these datasets, we also report in Appendix A results for CITIBIKE, a data set consisting of rental events from a bike sharing service in New York City.

**Results** To evaluate the capability of our proposed models, we compare against commonly-used baselines and state-of-the models. In some settings, ground intensity and conditional mark density are independent of each other and we can freely combine different baselines for the temporal and spatial domains. As temporal baselines, we use a homogeneous Poisson process, a self-correction process, and a Hawkes process. As spatial baselines, we use a conditional kernel density estimator (KDE), where  $p(\mathbf{x}|t)$  is essentially modeled as a history-dependent Gaussian mixture model (see Appendix B), as well as the Time-varying CNF (see section 3). In addition, we also compare to our implementation of Neural Jump SDEs ([Jia & Benson, 2019](#)) where the spatial distribution is a Gaussian mixture model, but we improve the architecture to use our GRU-based continuous-time hidden states for fair comparison, as we found the simpler parameterization in [Jia & Benson \(2019\)](#) to be numerically unstable for long sequences.

The results of our evaluation are shown in table 1. It can be seen that our proposed neural STPPs achieve strong results and typically outperform the comparison models by a large margin. Across all data sets, the Time-varying CNF outperforms the conditional KDE baseline despite not being conditional on history. This suggests that the overall spatial distribution is rather complex and cannot be modeled with simple Gaussian clusters. On PINWHEEL and EARTHQUAKES, the history-dependent Jump and Attentive CNF models achieve substantially better log-likelihoods in both the temporal and spatial domain. For COVID-19, the self-exciting Hawkes process is a strong baseline — which aligns with similar results for other infectious diseases ([Park et al., 2019](#)) — but the neural STPPs achieve again substantially better spatial likelihoods.



---

When compared to Neural Jump SDEs (Jia & Benson, 2019), our proposed models show similar strong performance. First, it can be seen that on all datasets our models show far better spatial results which illustrates the benefits from using expressive CNFs for the spatial domain. Second, since our realization of Neural Jump SDEs and our STPPs use the same architecture to model the temporal domain, their temporal likelihoods are often close. However, there is still a statistically significant difference between Neural STPPs and Neural Jump SDEs even for the temporal log-likelihood, most notable on the BOLD5000 data set. This indicates that too restricted spatial models can negatively affect the temporal model since both domains are tightly coupled.

Finally, we note that the results of the Jump and Attentive CNFs are typically close; both achieving better spatial log-likelihoods compared to the Time-varying CNF which does not depend on event history. On EARTHQUAKES, COVID-19, and BOLD5000 the attentive model achieves even the best temporal or spatial likelihood, while being substantially faster to compute (see Appendix A for a runtime analysis).

## 6 CONCLUSION

To learn high-fidelity models of stochastic events occurring in continuous space and time, we have proposed a new class of parameterizations for spatio-temporal point processes. Our approach combines ideas of Neural Jump SDEs with Continuous Normalizing Flows and allows to retain the flexibility of neural temporal point processes while enabling highly expressive models of continuous marks. We leverage Neural ODEs as a computational method what allows to compute the exact likelihood of the joint model and show that our approach achieves state-of-the-art performance on spatio-temporal datasets collected from a wide range of domains.

One limitation of our method is currently that calls to ODE solvers can computationally be expensive and prevent thus the modeling of long sequences. Improvements to the scalability of Neural ODEs and RNN hybrids would benefit our approach substantially and are a very promising direction for future work. Another promising area for future work are applications of our method in earth and climate science which often are concerned with modeling highly complex spatio-temporal data. In this context, the use of Riemannian CNFs (Mathieu & Nickel, 2020; Lou et al., 2020) is also especially interesting as it allows us to model Neural STPPs on the sphere simply by replacing the CNF in our models with a Riemannian counterpart.

## ACKNOWLEDGMENTS

We acknowledge the Python community (Van Rossum & Drake Jr, 1995; Oliphant, 2007) for developing the core set of tools that enabled this work, including PyTorch (Paszke et al., 2019), torchdiffeq (Chen, 2018), Hydra (Yadan, 2019), fairseq (Ott et al., 2019), Jupyter (Kluyver et al., 2016), Matplotlib (Hunter, 2007), seaborn (Waskom et al., 2018), Cython (Behnel et al., 2011), numpy (Oliphant, 2006; Van Der Walt et al., 2011), pandas (McKinney, 2012), and SciPy (Jones et al., 2014).

## REFERENCES

- Adrian Baddeley, Imre Bárány, and Rolf Schneider. Spatial point processes and their applications. *Stochastic Geometry: Lectures Given at the CIME Summer School Held in Martina Franca, Italy, September 13–18, 2004*, pp. 1–75, 2007.
- Earvin Balderama, Frederic Paik Schoenberg, Erin Murray, and Philip W Rundel. Application of branching models in the study of invasive species. *Journal of the American Statistical Association*, 107(498):467–476, 2012.
- Stefan Behnel, Robert Bradshaw, Craig Citro, Lisandro Dalcin, Dag Sverre Seljebotn, and Kurt Smith. Cython: The best of both worlds. *Computing in Science & Engineering*, 13(2):31–39, 2011.
- Nadine Chang, John A Pyles, Austin Marcus, Abhinav Gupta, Michael J Tarr, and Elissa M Aminoff. BOLD5000, a public fMRI dataset while viewing 5000 visual images. *Scientific data*, 6(1):1–18, 2019.

- 
- Ricky T. Q. Chen. torchdiffeq, 2018. URL <https://github.com/rtqichen/torchdiffeq>.
- Ricky T. Q. Chen, Yulia Rubanova, Jesse Bettencourt, and David K. Duvenaud. Neural ordinary differential equations. In *Advances in neural information processing systems*, pp. 6571–6583, 2018.
- Kyunghyun Cho, Bart Van Merriënboer, Caglar Gulcehre, Dzmitry Bahdanau, Fethi Bougares, Holger Schwenk, and Yoshua Bengio. Learning phrase representations using RNN encoder-decoder for statistical machine translation. *arXiv preprint arXiv:1406.1078*, 2014.
- Daryl J Daley and David Vere-Jones. An introduction to the theory of point processes, volume 1: Elementary theory and methods. *Verlag New York Berlin Heidelberg: Springer*, 2003.
- Edward De Brouwer, Jaak Simm, Adam Arany, and Yves Moreau. GRU-ODE-Bayes: Continuous modeling of sporadically-observed time series. In *Advances in Neural Information Processing Systems*, pp. 7379–7390, 2019.
- Ruizhi Deng, Bo Chang, Marcus A Brubaker, Greg Mori, and Andreas Lehrmann. Modeling continuous stochastic processes with dynamic normalizing flows. *arXiv preprint arXiv:2002.10516*, 2020.
- Laurent Dinh, David Krueger, and Yoshua Bengio. Nice: Non-linear independent components estimation. *arXiv preprint arXiv:1410.8516*, 2014.
- Laurent Dinh, Jascha Sohl-Dickstein, and Samy Bengio. Density estimation using real nvp. 2016.
- Nan Du, Hanjun Dai, Rakshit Trivedi, Utkarsh Upadhyay, Manuel Gomez-Rodriguez, and Le Song. Recurrent marked temporal point processes: Embedding event history to vector. In *Proceedings of the 22nd ACM SIGKDD International Conference on Knowledge Discovery and Data Mining*, pp. 1555–1564, 2016.
- Chris Finlay, Jörn-Henrik Jacobsen, Levon Nurbekyan, and Adam M Oberman. How to train your neural ode. *arXiv preprint arXiv:2002.02798*, 2020.
- Will Grathwohl, Ricky T. Q. Chen, Jesse Bettencourt, and David Duvenaud. Scalable reversible generative models with free-form continuous dynamics. In *International Conference on Learning Representations*, 2019.
- Amanda S Hering, Cynthia L Bell, and Marc G Genton. Modeling spatio-temporal wildfire ignition point patterns. *Environmental and Ecological Statistics*, 16(2):225–250, 2009.
- Chin-Wei Huang, David Krueger, Alexandre Lacoste, and Aaron Courville. Neural autoregressive flows. In *International Conference on Machine Learning*, pp. 2078–2087, 2018.
- Chin-Wei Huang, Laurent Dinh, and Aaron Courville. Solving ode with universal flows: Approximation theory for flow-based models. In *ICLR 2020 Workshop on Integration of Deep Neural Models and Differential Equations*, 2020.
- John D Hunter. Matplotlib: A 2d graphics environment. *Computing in science & engineering*, 9(3): 90, 2007.
- Michael F Hutchinson. A stochastic estimator of the trace of the influence matrix for Laplacian smoothing splines. *Communications in Statistics-Simulation and Computation*, 19(2):433–450, 1990.
- Junteng Jia and Austin R Benson. Neural jump stochastic differential equations. In *Advances in Neural Information Processing Systems*, pp. 9847–9858, 2019.
- Eric Jones, Travis Oliphant, and Pearu Peterson. {SciPy}: Open source scientific tools for {Python}. 2014.
- Hyunjik Kim, George Papamakarios, and Andriy Mnih. The Lipschitz constant of self-attention. *arXiv preprint arXiv:2006.04710*, 2020.

- 
- Thomas Kluyver, Benjamin Ragan-Kelley, Fernando Pérez, Brian E Granger, Matthias Bussonnier, Jonathan Frederic, Kyle Kelley, Jessica B Hamrick, Jason Grout, Sylvain Corlay, et al. Jupyter notebooks-a publishing format for reproducible computational workflows. In *ELPUB*, pp. 87–90, 2016.
- Zhifeng Kong and Kamalika Chaudhuri. The expressive power of a class of normalizing flow models. *arXiv preprint arXiv:2006.00392*, 2020.
- Yang Li, Haidong Yi, Christopher M Bender, Siyuan Shan, and Junier B Oliva. Exchangeable neural ode for set modeling. *arXiv preprint arXiv:2008.02676*, 2020.
- Aaron Lou, Derek Lim, Isay Katsman, Leo Huang, Qingxuan Jiang, Ser-Nam Lim, and Christopher De Sa. Neural manifold ordinary differential equations. *arXiv preprint arXiv:2006.10254*, 2020.
- Emile Mathieu and Maximilian Nickel. Riemannian continuous normalizing flows. *arXiv preprint arXiv:2006.10605*, 2020.
- Wes McKinney. *Python for data analysis: Data wrangling with Pandas, NumPy, and IPython*. ” O’Reilly Media, Inc.”, 2012.
- Nazanin Mehrasa, Ruizhi Deng, Mohamed Osama Ahmed, Bo Chang, Jiawei He, Thibaut Durand, Marcus Brubaker, and Greg Mori. Point process flows. *arXiv preprint arXiv:1910.08281*, 2019.
- Hongyuan Mei and Jason Eisner. The Neural Hawkes Process: A neurally self-modulating multivariate point process. In *Advances in Neural Information Processing Systems 30: Annual Conference on Neural Information Processing Systems 2017, 4-9 December 2017, Long Beach, CA, USA*, pp. 6754–6764, 2017.
- Sebastian Meyer, Johannes Elias, and Michael Höhle. A space–time conditional intensity model for invasive meningococcal disease occurrence. *Biometrics*, 68(2):607–616, 2012.
- Jesper Moller and Rasmus Plenge Waagepetersen. *Statistical inference and simulation for spatial point processes*. CRC Press, 2003.
- Maximilian Nickel and Matthew Le. Learning multivariate hawkes processes at scale. *arXiv preprint arXiv:2002.12501*, 2020.
- Yosihiko Ogata. Statistical models for earthquake occurrences and residual analysis for point processes. *Journal of the American Statistical association*, 83(401):9–27, 1988.
- Yosihiko Ogata. Space-time point-process models for earthquake occurrences. *Annals of the Institute of Statistical Mathematics*, 50(2):379–402, 1998.
- Travis E Oliphant. *A guide to NumPy*, volume 1. Trelgol Publishing USA, 2006.
- Travis E Oliphant. Python for scientific computing. *Computing in Science & Engineering*, 9(3): 10–20, 2007.
- Myle Ott, Sergey Edunov, Alexei Baevski, Angela Fan, Sam Gross, Nathan Ng, David Grangier, and Michael Auli. fairseq: A fast, extensible toolkit for sequence modeling. In *Proceedings of the 2019 Conference of the North American Chapter of the Association for Computational Linguistics (Demonstrations)*, pp. 48–53, Minneapolis, Minnesota, June 2019. Association for Computational Linguistics. doi: 10.18653/v1/N19-4009. URL <https://www.aclweb.org/anthology/N19-4009>.
- T. Ozaki. Maximum likelihood estimation of Hawkes’ self-exciting point processes. *Annals of the Institute of Statistical Mathematics*, 31(1):145–155, Dec 1979. ISSN 1572-9052. doi: 10.1007/bf02480272.
- Junhyung Park, Adam W Chaffee, Ryan J Harrigan, and Frederic Paik Schoenberg. A non-parametric Hawkes model of the spread of ebola in west africa. 2019.

- 
- Adam Paszke, Sam Gross, Francisco Massa, Adam Lerer, James Bradbury, Gregory Chanan, Trevor Killeen, Zeming Lin, Natalia Gimelshein, Luca Antiga, et al. Pytorch: An imperative style, high-performance deep learning library. In *Advances in neural information processing systems*, pp. 8026–8037, 2019.
- Prajit Ramachandran, Barret Zoph, and Quoc V Le. Searching for activation functions. *arXiv preprint arXiv:1710.05941*, 2017.
- Alex Reinhart et al. A review of self-exciting spatio-temporal point processes and their applications. *Statistical Science*, 33(3):299–318, 2018.
- Davis Rempe, Tolga Birdal, Yongheng Zhao, Zan Gojcic, Srinath Sridhar, and Leonidas J Guibas. CaSPR: Learning canonical spatiotemporal point cloud representations. *arXiv preprint arXiv:2008.02792*, 2020.
- Daniilo Rezende and Shakir Mohamed. Variational inference with normalizing flows. In *International Conference on Machine Learning*, pp. 1530–1538, 2015.
- Yulia Rubanova, Ricky T. Q. Chen, and David Duvenaud. Latent ODEs for irregularly-sampled time series. *arXiv preprint arXiv:1907.03907*, 2019.
- Frederic Paik Schoenberg, Marc Hoffmann, and Ryan J Harrigan. A recursive point process model for infectious diseases. *Annals of the Institute of Statistical Mathematics*, 71(5):1271–1287, 2019.
- Oleksandr Shchur, Marin Biloš, and Stephan Günnemann. Intensity-free learning of temporal point processes. *arXiv preprint arXiv:1909.12127*, 2019.
- John Skilling. The eigenvalues of mega-dimensional matrices. In *Maximum Entropy and Bayesian Methods*, pp. 455–466. Springer, 1989.
- Enzo Tagliazucchi, Pablo Balenzuela, Daniel Fraiman, and Dante R Chialvo. Criticality in large-scale brain fMRI dynamics unveiled by a novel point process analysis. *Frontiers in physiology*, 3:15, 2012.
- Enzo Tagliazucchi, Michael Siniatchkin, Helmut Laufs, and Dante R Chialvo. The voxel-wise functional connectome can be efficiently derived from co-activations in a sparse spatio-temporal point-process. *Frontiers in neuroscience*, 10:381, 2016.
- Takeshi Teshima, Isao Ishikawa, Koichi Tojo, Kenta Oono, Masahiro Ikeda, and Masashi Sugiyama. Coupling-based invertible neural networks are universal diffeomorphism approximators. *arXiv preprint arXiv:2006.11469*, 2020.
- The New York Times. Coronavirus (Covid-19) Data in the United States, 2020. URL <https://github.com/nytimes/covid-19-data>.
- Alexander Tong, Jessie Huang, Guy Wolf, David van Dijk, and Smita Krishnaswamy. TrajectoryNet: A dynamic optimal transport network for modeling cellular dynamics. *arXiv preprint arXiv:2002.04461*, 2020.
- U.S. Geological Survey. Earthquake Catalogue (accessed August 21, 2020), 2020. URL <https://earthquake.usgs.gov/earthquakes/search/>.
- Stefan Van Der Walt, S Chris Colbert, and Gael Varoquaux. The numpy array: a structure for efficient numerical computation. *Computing in Science & Engineering*, 13(2):22, 2011.
- Guido Van Rossum and Fred L Drake Jr. *Python reference manual*. Centrum voor Wiskunde en Informatica Amsterdam, 1995.
- Ashish Vaswani, Noam Shazeer, Niki Parmar, Jakob Uszkoreit, Llion Jones, Aidan N Gomez, Łukasz Kaiser, and Illia Polosukhin. Attention is all you need. In *Advances in neural information processing systems*, pp. 5998–6008, 2017.

---

Michael Waskom, Olga Botvinnik, Drew O’Kane, Paul Hobson, Joel Ostblom, Saulius Lukauskas, David C Gemperline, Tom Augspurger, Yaroslav Halchenko, John B. Cole, Jordi Warmenhoven, Julian de Ruyter, Cameron Pye, Stephan Hoyer, Jake Vanderplas, Santi Villalba, Gero Kunter, Eric Quintero, Pete Bachant, Marcel Martin, Kyle Meyer, Alistair Miles, Yoav Ram, Thomas Brunner, Tal Yarkoni, Mike Lee Williams, Constantine Evans, Clark Fitzgerald, Brian, and Adel Qalieh. `mwaskom/seaborn: v0.9.0` (july 2018), July 2018. URL <https://doi.org/10.5281/zenodo.1313201>.

Omry Yadan. Hydra - a framework for elegantly configuring complex applications. Github, 2019. URL <https://github.com/facebookresearch/hydra>.

Guandao Yang, Xun Huang, Zekun Hao, Ming-Yu Liu, Serge Belongie, and Bharath Hariharan. PointFlow: 3d point cloud generation with continuous normalizing flows. In *Proceedings of the IEEE International Conference on Computer Vision*, pp. 4541–4550, 2019.



## A ADDITIONAL RESULTS

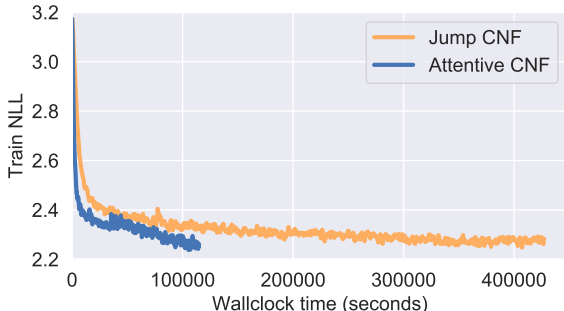


Figure 7: Runtime comparison of Jump and Attentive CNF.

Model	Citibike NY	
	Temporal	Spatial
Poisson Process	0.6092 $\pm$ 0.0123	–
Self-correcting Process	-5.6494 $\pm$ 1.4328	–
Hawkes Process	1.062 $\pm$ 0.0001	–
Conditional KDE	–	-2.856 $\pm$ 0.000
Time-varying CNF	–	-2.132 $\pm$ 0.012
Neural Jump SDE	1.092 $\pm$ 0.002	-2.731 $\pm$ 0.001
Jump CNF	1.105 $\pm$ 0.002	-2.155 $\pm$ 0.015
Attentive CNF	1.112 $\pm$ 0.002	-2.095 $\pm$ 0.006

Table 2: Log-likelihood values on held-out test data.

## B BASELINE

Our self-excitation baseline uses a Hawkes process to model the temporal variable, then uses a Gaussian mixture model to describe the spatial distribution conditioned on history of events. This corresponds to the following likelihood decomposition

$$\log p(t_1, \dots, t_n, x_1, \dots, x_n) = \sum_{i=1}^n \log p(x_i | t_i, t_1, \dots, t_{i-1}, x_1, \dots, x_{i-1}) + \sum_{i=1}^n \log p(t_i | t_1, \dots, t_{i-1}) \quad (20)$$

This dependence structure allows the usage of simple temporal point processes to model  $t_i$ , e.g. a Hawkes process, since temporal variables do not depend on the spatial information. The spatial distribution conditions all past events as well as the current time of occurrence.

Our baseline model assumes a simple Gaussian conditional model, that new events are likely to appear near previous events.

$$\log p(x_i | t_i, t_1, \dots, t_{i-1}, x_1, \dots, x_{i-1}) = \sum_{j=1}^{i-1} \alpha_j \mathcal{N}(x_j | \sigma^2), \quad \alpha_j = \frac{\exp\{(t_j - t_i)/\tau\}}{\sum_{j'=1}^{i-1} \exp\{(t_{j'} - t_i)/\tau\}} \quad (21)$$

This parametric model has two learnable parameters:  $\sigma^2$  and  $\tau$ , which control the rate of decay in the spatial and temporal domains, respectively.

However, this Gaussian spatial model assumes events are propagated in all directions equally and can only model local self-excitation behavior. These assumptions are often suitable for simplicity but are generally incorrect for many spatio-temporal data. To name a few, earthquakes occur more frequently along boundaries of tectonic plates, epidemics propagate along traffic routes, taxi demands saturate locally and change as customers move around.

## C PRE-PROCESSING STEPS FOR EACH DATA SET

**EARTHQUAKES** For modeling earthquakes and aftershocks, we gathered location and time of all earthquakes in Japan from 1990 to 2020 with magnitude of at least 2.5 from the [U.S. Geological Survey \(2020\)](#). We removed earthquakes from 2010 November to 2011 December, as these sequences were too long and only served as outliers in the data. Starting from January 01, 1990, we created sequences with a gap of 7 days. Each sequence was of length 30 days. We ensured there was no contamination between train/val/test sets by removing intermediate sequences. This resulted in 950 training sequences, 50 validation sequences, and 50 test sequences.

**COVID-19 CASES** We use data released publicly by [The New York Times \(2020\)](#) on daily COVID-19 cases in the New Jersey state, from March to July of 2020. The data is aggregated at the county level, which we dequantize uniformly across the county. We also dequantize the temporal axis by assigning new cases uniformly within the day. Starting at March 15, and every 3 days, we took a 7 day length

sequence. For each sequence, we sampled each event with a probability of 0.01. This was done 50 times per sequence. We ensured there was no contamination between train/val/test sets by removing intermediate sequences. This resulted in 1450 training sequences, 100 validation sequences, and 100 test sequences.

**CITIBIKE** Citibike is a bike sharing service in New York City. We treat the start of each trip as an event, and use the data from April to August of 2019. We split into sequences of length 1 day starting at 5:00am of each day. For each sequence, we subsampled with a probability of 0.005 per event, 20 times. This resulted in 2440 training sequences, 300 validation sequences, and 320 test sequences.

**BOLD5000** This consists of fMRI scans of four participants as they are given visual stimuli (Chang et al., 2019). We use the sessions of a single patient and for each run, we split into 3 sequences, treated individually. We converted brain responses into spatio-temporal events following the z-score thresholding approach in Tagliazucchi et al. 2016, Equation (2). We used a threshold of  $\gamma = 6.0$ . We split the data into 1050 training sequences, 150 val sequences, 220 test sequences.

## D HYPERPARAMETERS CHOSEN AND TESTED

For the time-varying, jump, and attentive CNF models, we parameterized the CNF drift as a multilayer perceptron (MLP) with dimensions  $[d - 64 - 64 - 64 - d]$ , where  $d$  is the number of spatial variables. We swept over activation functions between using softplus or a time-dependent Swish (Ramachandran et al., 2017).

$$\text{TimeDependentSwish}(t, z) = h\sigma(\beta(t) \odot z) \quad (22)$$

where  $\sigma$  is the logistic sigmoid function,  $\odot$  is the Hadamard (element-wise) product, and  $\beta : \mathbb{R} \rightarrow \mathbb{R}_{d_z}$  is a MLP with widths  $[1 - 64 - d_z]$  where  $d_z$  is the dimension of  $z$ , using the softplus activation function. We ultimately decided on using the time-dependent Swish for all experiments.

We swept over the MLP for defining  $f_h$  for the continuous-time hidden state in eq. (11) using hidden widths of  $[8 - 20]$ ,  $[32 - 32]$ ,  $[64 - 64]$ ,  $[32 - 32 - 32]$ , and  $[64 - 64 - 64]$ . The majority of models used  $32 - 32$  as it provided enough flexibility while remaining easy to solve. We used the softplus activation function. We tried MLP for parameterizing the instantaneous change in eq. (12); however, it was too unstable for long sequences. We therefore switched to the GRU parameterization. We regularized the  $L_2$  norm of the hidden state drift with a strength of  $1e-4$ , chosen from  $\{0, 1e-4, 1e-3, 1e-2\}$ . We optionally used optimal transport-inspired regularization from Finlay et al. (2020), which adds a Frobenius norm regularization to the gradient of the drift in addition to the  $L_2$  norm regularization, to the CNF models with a strength of  $\{0, 1e-4, 1e-3, 1e-2\}$ . The Time-varying and Attentive CNF models did not require regularization and were mostly kept at 0, but the Jump CNF models benefited from some amount of regularization to avoid numerical instability.

For the Jump CNF, we used a composition of 4 radial flows (Rezende & Mohamed, 2015) to parameterize the instantaneous updates in eq. (17). All parameters of the radial flows were parameterized to be the output of a MLP that takes as input the hidden state at the time of the event (before the hidden state is updated based on the current event). The radial flows were initialized in such a way that the log determinant is near zero.

For the Attentive CNF, we tested both standard multihead attention (Vaswani et al., 2017) and the Lipschitz multihead attention (Kim et al., 2020). The Lipschitz multihead attention typically produced similar validation NLL as the standard multihead attention but were more stable on multiple occasions. We therefore kept the Lipschitz multihead attention for all experiments.

We initialized all Neural ODEs (for the hidden state and CNFs) with zero drift.

## E REMOVING CROSS-EVENT PARTIAL DERIVATIVES

This results in a lower-variance gradient estimator for training, and allows parallel computation of conditional log probabilities at test time.

We first summarily describe the attention mechanism. For an input  $X \in \mathbb{R}^{n \times d}$  representing the sequence of  $n$  variables  $\{x_s^{(0)}, \dots, x_s^{(n)}\}$  at some value of  $s$ , this attention mechanism creates logits

---

$P \in \mathbb{R}^{n \times n}$  and values  $V \in \mathbb{R}^{n \times d}$ , both dependent on  $X$ , such that the output is

$$O = \underbrace{\text{softmax}(P)}_{:=S} V. \quad (23)$$

where the softmax is taken over each row of  $P$ . The output is then added to  $X$  as a residual connection. The multihead attention computes  $P$  in a way such that  $P_{ij}$  depends on  $X_i$  and  $X_j$ , and  $V_i$  depends on  $X_i$ . This is true for both the vanilla MHA (Vaswani et al., 2017) and the L2 MHA (Kim et al., 2020). For our use case,  $P_{ij}$  is set to  $-\text{inf}$  for  $j > i$  as we don't want to attend to future events.

We retain only the block-diagonal gradients where each block contains variables corresponding to one event. This is equivalent to removing all the cross-event dependencies.

$$\frac{\partial O_i}{\partial X_i} = S_{:,i} \frac{\partial V_i}{\partial X_i} + V^\top \frac{\partial S}{\partial P_i} \frac{\partial P_i}{\partial X_i} + V^\top \frac{\partial S}{\partial P_{:,i}} \frac{\partial P_{:,i}}{\partial X_i} \quad (24)$$

See released code for implementation.